

Wide-field cosmic shear surveys

Mellier Y.^{a,b,c}, van Waerbeke L.^a, Bertin E.^{a,b,c}, Tereno I.^a and F. Bernardreau^c

^aIAP, 98 bis Blvd Arago, 75014 Paris, France

^bObs. de Paris/LERMA, 77 Av. Denfert-Rochereau, 75014 Paris, France

^cTERAPIX-IAP, 98 bis Blvd Arago, 75014 Paris, France

^dSPhT, CE Saclay, 91191 Gif sur Yvette cedex, France.

ABSTRACT

We present the current status of cosmic shear based on all surveys done so far. Taken together, they cover more about 70 deg² and concern more than 3 million galaxies with accurate shape measurement. Theoretical expectations, observational results and their cosmological interpretations are discussed in the framework of standard cosmology and CDM scenarios. The potentials of the next generation cosmic shear surveys are discussed.

Keywords: Cosmology, Large Scale Structure, Gravitational Lensing, Weak Lensing, Surveys

1. INTRODUCTION

Gravitational lensing produces distortion of light beams which modifies the image shapes of background galaxies. In a Friedman-Robertson-Walker metric, and for stationary, weak gravitational fields, the deflection angle writes

$$\hat{\alpha} = \frac{2}{c^2} \int \nabla_{\perp} \Phi \, dl , \quad (1)$$

where c is the celerity and Φ the 3-dimension gravitational potential. In general, the deflection angle is small and lenses can be approximated as thin gravitational systems. This simplifies the relation between the source (S) and image (I) positions according to the simple geometrical “lens equation”:

$$\theta^I = \theta^S + \frac{D_{LS}}{D_{OS}} \hat{\alpha}(\theta^I) , \quad (2)$$

where D_{ij} are angular diameter distances.

Equations (1) and (2) express how lens properties depend on dark matter distribution and on cosmological models. From an observational point of view, gravitational lenses manifest as image multiplication of galaxies or quasars, strong and weak distortions of galaxy shape or transient micro-lensing effects. These effects, as well as the time delays attached to image multiplications are exploited in order to probe the geometry and matter/energy content of the Universe or to observe high-redshift galaxies (see 1, 2, 3, 4 for reviews) .

In the case of weak gravitational lensing, useful approximations relating observed shapes of galaxies to gravitational shear can be made. In general, the image magnification is characterized by the convergence, κ , and by the shear components γ_1 and γ_2 :

$$\kappa = \frac{1}{2} (\varphi_{,11} + \varphi_{,22}); \quad \gamma_1(\theta) = \frac{1}{2} (\varphi_{,11} - \varphi_{,22}); \quad \gamma_2(\theta) = \varphi_{,12} = \varphi_{,21} \quad (3)$$

where the $\varphi_{,ij}$ are the second derivatives of φ with respect to the i, j coordinates and

$$\varphi(\theta) = \frac{2}{c^2} \frac{D_{LS}}{D_{OS} D_{OL}} \int \Phi(D_{OL}\theta, z) \, dz . \quad (4)$$

Further author information: (Send correspondence to Y. Mellier)
Y. Mellier: E-mail: mellier@iap.fr, Telephone: (+33) 1 44 32 81 40

The shear applied to lensed galaxies increases their ellipticity along a direction perpendicular to the gradient of the projected potential. The lens-induced distortion $\boldsymbol{\delta}$ can then be evaluated from the shape of galaxies as it can be observed from the components of their surface brightness second moment $M_{ij} = \frac{\int I(\boldsymbol{\theta}) \theta_i \theta_j d^2\theta}{\int I(\boldsymbol{\theta}) d^2\theta}$:

$$\boldsymbol{\delta} = \frac{2\gamma (1 - \kappa)}{(1 - \kappa)^2 + |\gamma|^2} = \left(\delta_1 = \frac{M_{11} - M_{22}}{Tr(M)} ; \delta_2 = \frac{2M_{12}}{Tr(M)} \right). \quad (5)$$

In the weak lensing regime, the relation between the distortion and the gravitational shear simplifies to $\boldsymbol{\delta} \approx 2\gamma$, so in principle ellipticity of galaxies, as measured from the second moment components, provides a direct estimate of the gravitational shear. The “shear map” can then be used to reconstruct the “mass map” at any galaxy position. However, since each galaxy has its own intrinsic ellipticity, and since the background galaxies only sparsely sample the sky, the final shear-induced ellipticity map is contaminated by shot noise and cannot have infinite resolution.

The use of ellipticities of galaxies for weak lensing statistics has three important applications: galaxy-galaxy lensing, mass reconstruction of clusters of galaxies and gravitational distortion induced by large-scale structures of the universe. Each permits to recover properties of the dark matter located in gravitational systems as well as the mass density of the universe. In the following we only focus on weak lensing analysis applied to large-scale structures, namely the cosmic shear.

2. MOTIVATIONS FOR COSMIC SHEAR SURVEYS

Cosmic shear refers to the weak distortion of light bundles produced by the cumulative effects of mass inhomogeneities in the universe. Although theoretical cosmological weak lensing studies started more than 30 years ago, it is only recently that this topic moved to an observational cosmology tool. Progresses in the field are going incredibly fast, despite observational and technical difficulties, and put cosmic shear as CMB was only few years ago. These remarkable progresses were possible because wide field surveys with panoramic CCD cameras grow rapidly and can be handled with present-day computing facilities.

Light propagation through an inhomogeneous universe accumulates weak lensing effects over Gigaparsec distances. Assuming structures formed from gravitational growth of Gaussian fluctuations, the shape and amplitude of cosmological weak lensing as function of angular scale can be predicted from Perturbation Theory. To first order, the convergence $\kappa(\boldsymbol{\theta})$ at angular position $\boldsymbol{\theta}$ is given by the line-of-sight integral

$$\kappa(\boldsymbol{\theta}) = \frac{3}{2} \Omega_0 \int_0^{z_s} n(z_s) dz_s \int_0^{\chi(z_s)} \frac{D(z, z_s) D(z)}{D(z_s)} \delta(\chi, \boldsymbol{\theta}) [1 + z(\chi)] d\chi \quad (6)$$

where $\chi(z)$ is the radial distance out to redshift z , D the angular diameter distances, $n(z_s)$ is the redshift distribution of the sources. δ is the mass density contrast responsible for the deflection at redshift z . Its amplitude at a given redshift depends on the properties of the (dark) matter power spectrum and its evolution with look-back-time.

The cumulative weak lensing effects of structures induce a shear field which is primarily related to the power spectrum of the projected mass density, P_κ . Its statistical properties can be recovered by the shear top-hat variance (10, 19, 21),

$$\langle \gamma^2 \rangle = \frac{2}{\pi \theta_c^2} \int_0^\infty \frac{dk}{k} P_\kappa(k) [J_1(k\theta_c)]^2, \quad (7)$$

the aperture mass variance (22, 24)

$$\langle M_{\text{ap}}^2 \rangle = \frac{288}{\pi \theta_c^4} \int_0^\infty \frac{dk}{k^3} P_\kappa(k) [J_4(k\theta_c)]^2, \quad (8)$$

and the shear correlation function (10, 19, 21):

$$\langle \gamma \gamma \rangle_\theta = \frac{1}{2\pi} \int_0^\infty dk k P_\kappa(k) J_0(k\theta), \quad (9)$$

where J_n is the Bessel function of the first kind. $P_\kappa(k)$ is directly related to the 3-dimension power spectrum of the dark matter along the line of sight, P_{3D} :

$$P_\kappa(k) = \frac{9}{4} \Omega_m^2 \int_0^\infty P_{3D} \left(\frac{k}{D_L(z)}, z \right) W(z, z_s) dz, \quad (10)$$

where $W(z, z_s)$ is an efficiency function which depends on the redshift distribution of sources and lenses. Therefore, in principle an inversion permit to reconstruct the 3-dimension power spectrum of the dark matter from the weak distortion field.

Higher order statistics, like the skewness of the convergence, $s_3(\theta)$, can also be computed. They probe non Gaussian features in the projected mass density field, like massive clusters or compact groups of galaxies (5' 6). The amplitude of cosmic shear signal and its sensitivity to cosmology can be illustrated in the fiducial case of a power law mass power spectrum with no cosmological constant and a background population at a single redshift z . In that case $\langle \kappa(\theta)^2 \rangle$ and $s_3(\theta)$ write:

$$\langle \kappa(\theta)^2 \rangle^{1/2} = \langle \gamma(\theta)^2 \rangle^{1/2} \approx 1\% \sigma_8 \Omega_m^{0.75} z_s^{0.8} \left(\frac{\theta}{1'} \right)^{-\left(\frac{n+2}{2}\right)}, \quad (11)$$

and

$$s_3(\theta) = \frac{\langle \kappa^3 \rangle}{\langle \kappa^2 \rangle^2} \approx 40 \Omega_m^{-0.8} z_s^{-1.35}, \quad (12)$$

where n is the spectral index of the power spectrum of density fluctuations. Therefore, in principle the degeneracy between Ω_m and σ_8 can be broken when both the variance and the skewness of the convergence are measured.

3. DETECTION OF WEAK DISTORTION SIGNAL

3.1. An observational challenge

Eq. (11) shows that the amplitude of weak lensing signal is of the order of few percents, which is much smaller than the intrinsic dispersion of ellipticity distribution of galaxies. Adopting the null hypothesis that no gravitational weak lensing signal is present, we can predict the expected limiting shear if only shot noise and sampling are taken into account (in particular, we assume there is no systematic residual errors associated to image processing or PSF corrections as those discussed later). For a 3σ shear variance limiting detection it writes :

$$\langle \gamma(\theta)^2 \rangle_{limit}^{1/2} = 1.2\% \left[\frac{A_T}{1 \text{ deg}^2} \right]^{-\frac{1}{4}} \times \left[\frac{\sigma_{\epsilon_{gal}}}{0.4} \right] \times \left[\frac{n}{20 \text{ gal}/\text{arcmin}^2} \right]^{-\frac{1}{2}} \times \left[\frac{\theta}{10'} \right]^{-\frac{1}{2}}, \quad (13)$$

where A_T is the total area covered by the survey, $\sigma_{\epsilon_{gal}}$ is the intrinsic ellipticity dispersion of galaxy and n the galaxy number density of the survey. By comparing with Eq.(11) one concludes that a cosmic shear survey covering 1 deg^2 up to a reasonable depth corresponding to 20 gal./arcmin^2 should in principle be the minimum requirements to measure a cosmic shear signal. However, when gravitational shear is included these limits change as function of the angular scale and of cosmological parameters. Our simplistic estimate turns out to be too pessimistic on small scales because non-linear growth of perturbation producing clusters, groups and galaxies amplify the cosmic shear signal by a factor of 2 to 10, depending on cosmologies (5) . Van Waerbeke et al (7) explored which strategy would be best suited to probe statistical properties of such a small signal. Their results are illustrated on Table 1 and show that the variance of κ can already provide a valuable cosmological information, even with a survey covering about 1 deg^2 . However, for the skewness one needs at least 10 deg^2 . Furthermore, more than 100 deg^2 must be observed in order to uncover information on Ω_Λ or the shape of the power spectrum over scales larger than 1 degree.

The shape of objects may also be altered by atmospheric turbulence, optical and atmospheric distortions as well as unexpected telescope oscillations or CCD charge transfer efficiency. Non-cosmological signals reach amplitudes one order of magnitude higher than cosmic shear and removing them is indeed the most challenging

Table 1. Expected signal-to-noise ratio on the the variance and the skewness of the convergence for two cosmological models. In the first column, the size of the field of view (FOV) is given. The signal-to-noise ratio is computed from the simulations done by van Waerbeke et al (1999).

$z_s = 1$, Top Hat filter , $n = 30$ gal.arcmin $^{-2}$				
FOV (deg. \times deg.)	S/N Variance		S/N Skewness	
	$\Omega_m = 1$	$\Omega_m = 0.3$	$\Omega_m = 1$	$\Omega_m = 0.3$
1.3 \times 1.3	7	5	1.7	2
2.5 \times 2.5	11	10	2.9	4
5.0 \times 5.0	20	20	5	8
10.0 \times 10.0	35	42	8	17

Table 2. Present status of cosmic shear surveys with published results.

Telescope	Pointings	Total Area	Lim. Mag.	Ref..
CFHT	5 \times 30' \times 30'	1.7 deg 2	I=24.	9[vWME+]
CTIO	3 \times 40' \times 40'	1.5 deg 2	R=26.	11[WTK+]
WHT	14 \times 8' \times 15'	0.5 deg 2	R=24.	12[BRE]
CFHT	6 \times 30' \times 30'	1.0 deg 2	I=24.	14[KWL]
VLT/UT1	50 \times 7' \times 7'	0.6 deg 2	I=24.	15[MvWM+]
HST/WFPC2	1 \times 4' \times 42'	0.05 deg 2	I=27.	16
CFHT	4 \times 120' \times 120'	6.5 deg 2	I=24.	17[vWMR+]
HST/STIS	121 \times 1' \times 1'	0.05 deg 2	V \approx 26	27
CFHT	5 \times 126' \times 140'	24. deg 2	R=23.5	28
CFHT	10 \times 126' \times 140'	53. deg 2	R=23.5	29
CFHT	4 \times 120' \times 120'	8.5 deg 2	I=24.	30
HST/WFPC2	271 \times 2.1 \times 2.1	0.36 deg 2	I=23.5	25
Keck+WHT	173 \times 2' \times 8'	1.6 deg 2	R=25	18
	+13 \times 16' \times 8'			
	7 \times 16' \times 16'			

issues of these surveys. Fortunately, these alterations also modify the shape of stars, hence lensing and non-lensing contributions to galaxy shapes can be separated. Over the past decades many works focussed on the corrections of non-lensing contributions. All follow the basic scheme shown in Figure 1, but use different star shape analyses and correction techniques (see 3 and 4 for comprehensive reviews). The reliability of artificial anisotropy corrections has been discussed and tested at length (8, 9, 12, 13). In particular, Erben et al (8) have demonstrated that the so-called KSB method (23) is able to correct PSF anisotropy very well and allows astronomers to detected cosmic shear amplitude down to 1% level with a 10% relative accuracy, even if the non-lensing contribution is as large as 10%.

3.2. Detection

As we discussed in the previous section, on scale significantly smaller than one degree, non-linear structures dominate and increase the amplitude of the lensing signal, making its measurement easier. Few teams started such surveys during the past years and succeeded to get a significant signal. Table 2 lists some published results. Since each group used different telescopes, adopted different observing strategy and used different data analysis techniques, one can figure out their reliability by comparing these surveys. Figure 2 show that they are all in very good agreement*. This is a convincing demonstration that the expected correlation of ellipticities is real.

*The Hoekstra et al (28) data are missing because depth is different so the sources are at lower redshift and the amplitude of the shear is not directly comparable to other data plotted

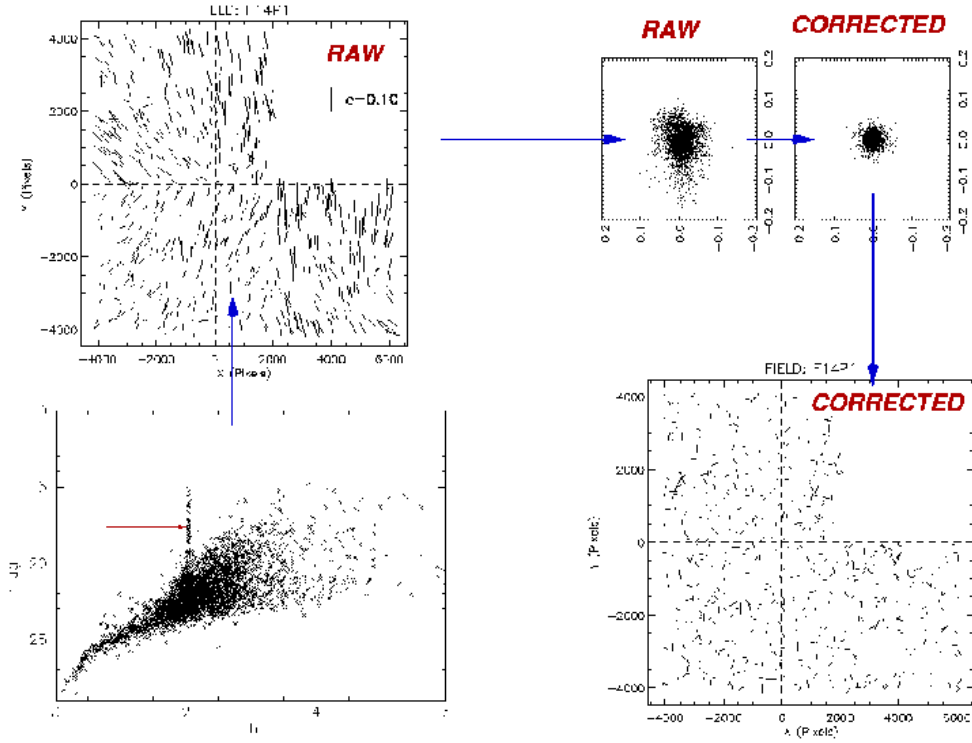


Figure 1. Basic scheme for the non-lensing distortion correction of cosmic shear surveys. Stars of each field are first selected in the vertical branch of the size-magnitude plots. The PSF (Raw) is then mapped over the whole field which permits to remove the non-lensing distortion anywhere in the field from simple interpolations. The corrected stars provide an estimated of the residual (Corrected).

3.3. Cosmological nature of the signal

The cosmological origin of the coherent distortion signal detected by all these surveys is not obvious. Even if a cosmological signal is present in the data, it could be strongly contaminated by unknown systematic contributions or residuals systematic errors produced by the PSF corrections discussed above. An elegant way to check whether corrections are correctly done and to confirm the gravitational nature of the signal is to decompose the signal into E- and B- modes. The E-mode is a gradient term which contains signal produced by gravity-induced distortion. On the other hand, the B-mode is a pure curl-component, so it only contains intrinsic ellipticity correlation or systematics residuals. Both modes have been extracted using the aperture mass statistics by van Waerbeke et al (17, 26) and Pen et al (30) in the VIRMOS-DESCART^{†‡} survey as well as by Hoekstra et al (29) in the Red Cluster Sequence survey. In both samples, the E-mode dominates the signal, although a small residual is detected in the B-mode on small scales for the RCS sample and on large scales for the VIRMOS-DESCART sample. These residuals still need further investigations. This strongly supports the gravitational origin of the distortion.

An alternative to a gravitational lensing origin to the signal could be an intrinsic correlations of ellipticities of galaxies produced by proximity effects (tidal torques). Several recent numerical and theoretical studies (31,

[†]For the VIRMOS spectroscopic survey, see (34). For the VIRMOS-DESCART survey see <http://terapix.iap.fr/Descart/>

[‡]Data of the VIRMOS-DESCART survey were processed and analysed at the TERAPIX data center: <http://terapix.iap.fr>

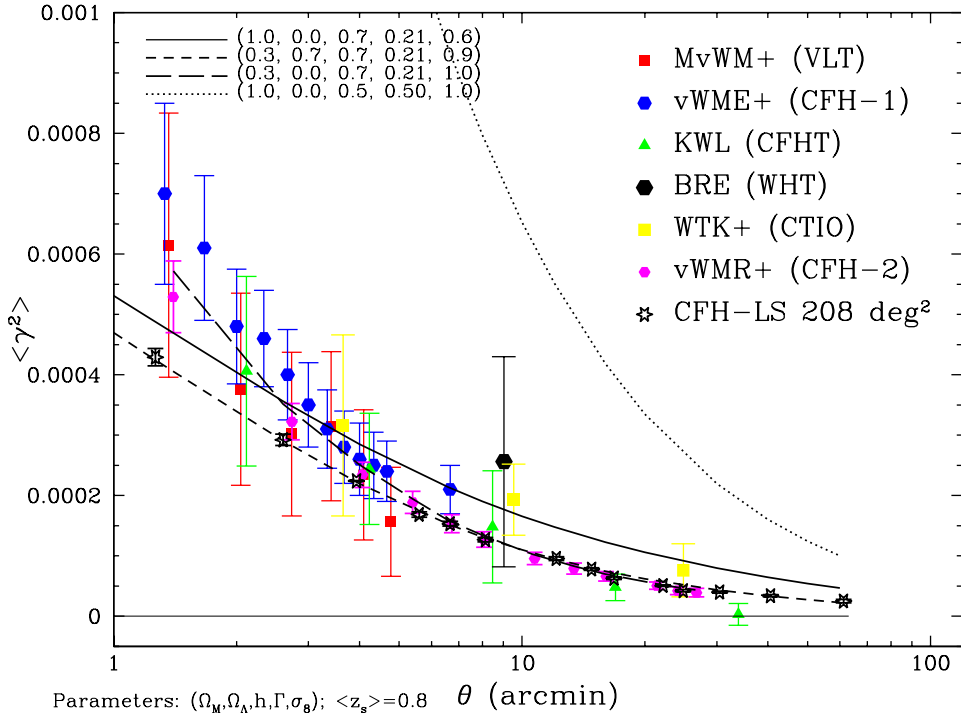


Figure 2. Top hat variance of shear as function of angular scale from 6 cosmic shear surveys. The acronyms of the right refer to the references reported in Table 2. The open black stars illustrate the expected performances of the CFHT-LS which will start by 2003 with Megacam at CFHT. This is the expected signal from the “Wide Survey” which will cover about 200 deg² up to $I_{AB} = 24.5$. As one can see, for most points the errors are smaller than the stars.

32) have addressed this point. From these first investigations, it seems that intrinsic correlations are negligible on scales beyond one arc-minute, provided the survey is deep enough, but this critical point is still debated. Nevertheless, we hope that deep surveys are reliable since in that case, most lensed galaxies along a line of sight are spread over Gigaparsec scales and have no physical relation with its apparent neighbors. Hence, since most cosmic survey are deep, we expect they are almost free of intrinsic correlations.

4. COSMOLOGICAL INTERPRETATIONS

4.1. 2-point statistics and variance

A comparison of the top-hat shear variance with some realistic cosmological models is plotted in Figure 2. Its amplitude has been scaled using photo- z which gives $\langle z \rangle \approx 1$. On this plot, we see that standard COBE-normalized CDM is ruled at a $10-\sigma$ confidence level. However, the degeneracy between Ω_m and σ_8 discussed in the previous section still hampers a strong discrimination among most popular cosmological models. The present-day constraints resulting from independent analyses by Maoli et al (15), Rhodes et al (16), van Waerbeke et al (17, 26), Hoekstra et al (28, 29) and Réfrégier et al (25) can be summarized by the following conservative boundaries (90% confidence level):

$$0.05 \leq \Omega_m \leq 0.8 \quad \text{and} \quad 0.5 \leq \sigma_8 \leq 1.2 , \quad (14)$$

and, in the case of a flat-universe with $\Omega_m = 0.3$, they lead to $\sigma_8 \approx 0.9$.

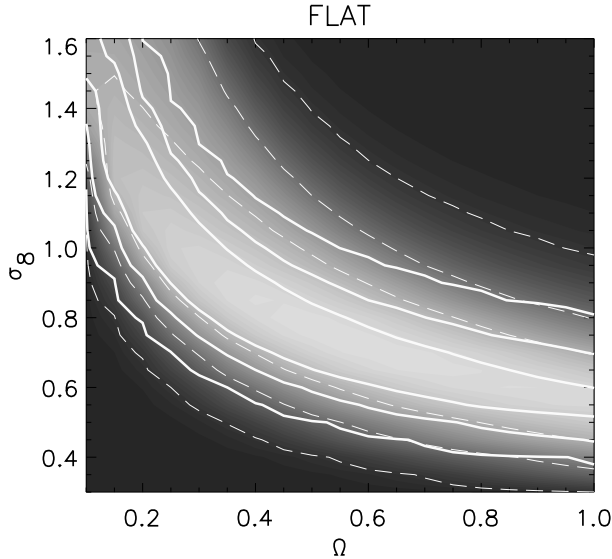


Figure 3. Constraints on Ω and σ_8 for the flat cosmologies. The confidence levels are [68, 95, 99.9] from the brightest to the darkest area. The gray area and the dashed contours correspond to the computations with a full marginalisation over the default prior $\Gamma \in [0.05, 0.7]$ and $z_s \in [0.24, 0.64]$. The thick solid line contours are obtained from the prior $\Gamma \in [0.1, 0.4]$ and $z_s \in [0.39, 0.54]$ (which is a mean redshift $\bar{z}_s \in [0.8, 1.1]$). From van Waerbeke et al. (2002) (26).

4.2. Toward breaking the $\Omega_m - \sigma_8$ degeneracy

The measurement of non-Gaussian features needs informations on higher order statistics than variance. Eq.(12) shows that the skewness of κ seems the best suited quantity for this purpose. However, in contrast with the variance, the skewness demands first to reconstruct the mass map of the field, which complicates the process. In fact, its measurements suffers from a number a practical difficulties which are not yet fixed. In particular, the masking process generates a Swiss-Cheese pattern over the field which significantly degrades the quality of the mass reconstruction and put strong doubts on the reliability of its skewness and its cosmological interpretation. Recently, Bernardeau, van Waerbeke & Mellier (37) have proposed an alternative method using some specific patterns in the shear three-point function. Despite the complicated shape of the three-point correlation pattern, they uncovered it can be used for the measurement of non-Gaussian features. Their detection strategy based on their method has been tested on ray tracing simulations and turns out to be robust, usable in patchy catalogs, and quite insensitive to the topology of the survey.

Bernardeau et al (38) used the analysis of the 3-point correlations function on the VIRMOS-DESCART data. Their results on Figure 4 show a 2.4σ signal over four independent angular bins, or equivalently, a 4.9σ confidence level detection with respect to measurements errors on scale of about 2 to 4 arc-minutes. The amplitude and the shape of the signal are consistent with theoretical expectations obtained from ray-tracing simulations. This result supports the idea that the measure corresponds to a cosmological signal due to the gravitational instability dynamics. Moreover, its properties could be used to put constraints on the cosmological parameters, in particular on the density parameter of the Universe. Although the errors are still large to permit secure conclusions, one clearly see that the amplitude and the shape of the 3-point correlations function match the most likely cosmological models. Remarkably, the Λ CDM scenario perfectly fit the data points.

The Bernardeau et al (38) result is the first detection of non-Gaussian features in a cosmic shear survey and it opens the route to break the $\Omega_m - \sigma_8$ degeneracy. Furthermore, this method is weakly dependent on other parameters, like the cosmological constant or the properties of the power spectrum. However, there are still some caveats which may be considered seriously. One difficulty is the source clustering which could significantly perturb high-order statistics (Hamana et al 2000 (33)). If so, multi-lens plane cosmic shear analysis will be necessary which implies a good knowledge of the redshift distribution. For very deep cosmic shear surveys which probe galaxies fainter than the limiting spectroscopic capabilities of 10-meter class telescopes, the lack

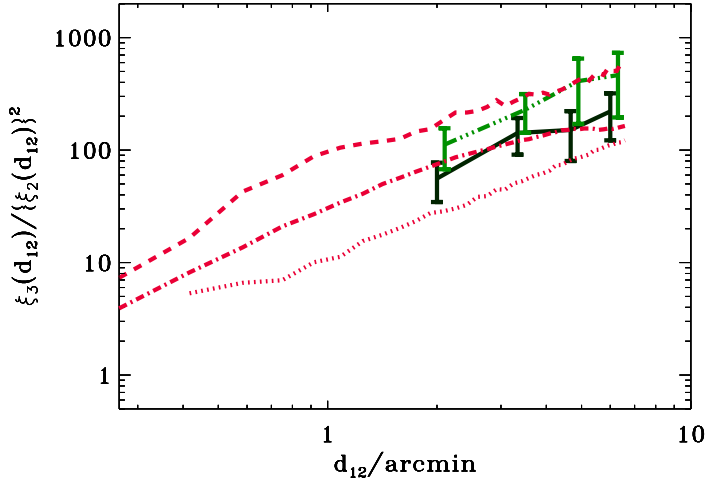


Figure 4. Results for the VIRMOS-DESCART survey of the reduced three point correlation function (38). The solid line with error bars shows the raw results, when both the E and B contributions to the two-point correlation functions are included. The dot-dashed line with error bars corresponds to measurements where the contribution of the B mode has been subtracted out from the two-point correlation function. These measurements are compared to results obtained in τ CDM, Λ CDM and Λ CDM simulations (dashed, dotted and dot-dashed lines respectively).

of reliable photometric redshift calibration be could be a serious concern.

5. OUTLOOK

Because on going surveys increase both in solid angle and in number of galaxies, they will quickly improve the accuracy of cosmic shear measurements, at a level where Ω_m and σ_8 will be known with a 10% accuracy. Since it is based on gravitational deflection by intervening matter spread over cosmological scales, the shape of the distortion field also probes directly the shape of the projected dark matter power spectrum. Pen et al (30) explored its properties by measuring for the first time the $C(l)$ of the dark matter (see Figure 5). Although the reliability of these $C(l)$ is still unknown, this work shows this is feasible with present data. The capabilities of cosmic shear surveys to probe dark matter can be also used to explore the relations between light and mass at different angular scale, different redshifts and in different environment. Recently Hoekstra et al (39) joined together the RCS and the VIRMOS-DESCART surveys and computed both the biasing and the galaxy-mass cross-correlation. They used the aperture mass and aperture number density statistics, as it was originally proposed by Schneider (35) and van Waerbeke (36). They found that the biasing is linear on scale beyond $3 h^{-1}$, but turns out to be more complex on lower scale, indicating a significant non-linear and/or stochastic biasing. These results are indeed difficult to interpret in a cosmological context without high resolution numerical simulations and a detailed scenario of galaxy formation in hands. But they show the remarkable potential of cosmic shear survey for challenging theory of galaxy formation against observations. Moreover, it is worth noticing that this work was made possible only because the two surveys merged their data in order to cover a sufficiently large field of view. The investigation of mass and light relations is certainly one of the most promising goals of wide cosmic shear surveys in the future.

However, we expect much more within the next decade. Several new wide field surveys are in progress at ESO/La Silla (Erben et al 2002 in preparation), at CTIO (Jarvis et al), at NOAO (Januzzi et al) and at SUBARU (Miyazaki 2002 (41)). Surveys covering hundreds of degrees, with multi-bands data in order to get redshift of sources and possibly detailed information of their clustering properties, are scheduled. The CFHT

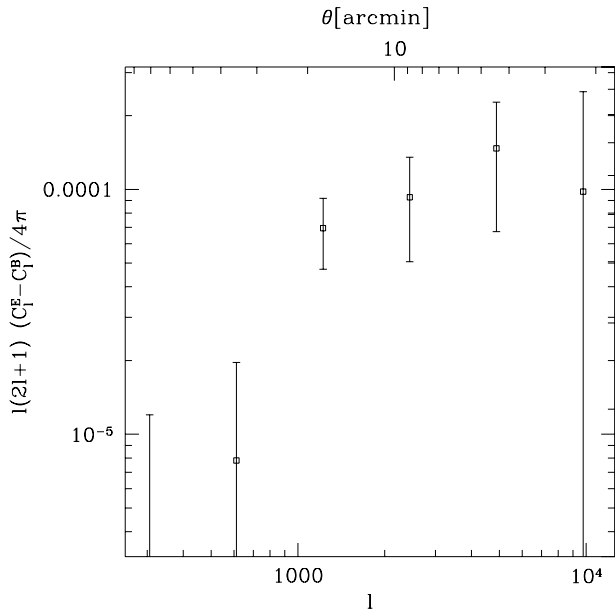


Figure 5. Cosmological results from cosmic shear surveys: The angular power spectrum of the convergence field from the VIRMOS-DESCART survey is plotted (From Pen et al 2001). These are the first $C(l)$ of dark matter ever measured in cosmology.

Legacy Survey[§] will cover 200 deg² and is one of those next-generation cosmic shear survey. Figures 1 and 6 shows their expected potential for cosmology. On figure 1 we simulated the expected signal to noise of the shear variance as function of angular scale for a Λ CDM cosmology. The error bars are considerably reduced as compared to present-day survey. On Fig. 6, we compare the expected signal to noise ratio of the CFHT Legacy Survey with the expected amplitude of the angular power spectrum for several theoretical quintessence fields models. It shows that even with 200 deg² which include multi-color informations in order to get redshift of sources, one can already obtain interesting constraints on cosmology beyond standard models.

The use of cosmic shear data can be much more efficient if they are used together with other surveys, like CMB (Boomerang, MAP, Planck), SNIa surveys, or even galaxy surveys (2dF, SDSS). For example, SDSS will soon provide the 100, 000 quasars with redshifts. Ménard & Bartelmann (42) have recently explored the interest of this survey in order to cross-correlate the foreground galaxy distribution with the quasar population. The expected magnification bias generated by dark matter associated with foreground structures as mapped by galaxies depends on Ω_m and the biasing σ_8 . In principle magnification bias in the SDSS quasar sample can provide similar constraints as cosmic shear. Both cosmic shear and cosmic magnification wide field surveys should soon produce impressive constraints on cosmological models.

Acknowledgements

We thank M. Bartelmann, R. Carlberg, T. Erben, B. Fort, H. Hoekstra, B. Jannuzzi, B., Ménard, O. Doré, U.-L. Pen, S. Prunet and P. Schneider for useful discussions. This work was supported by the TMR Network “Gravitational Lensing: New Constraints on Cosmology and the Distribution of Dark Matter” of the EC under contract No. ERBFMRX-CT97-0172.

REFERENCES

1. Blandford, R.D.; Narayan, R.; 1992 ARAA 30, 311.

[§]<http://www.cfht.hawaii.edu/Science/CFHLS/>

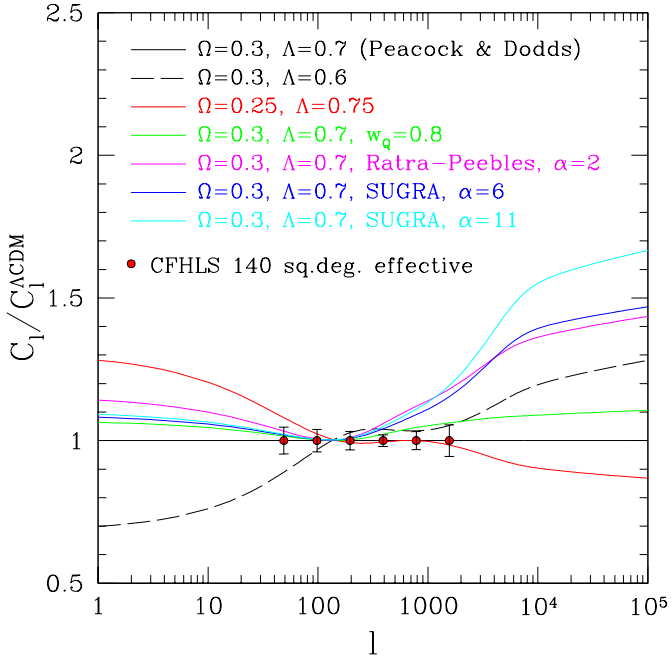


Figure 6. The future of from cosmic shear surveys: Theoretical expectations of the CFHT Legacy Survey. The dots with error bars are the expected measurements of cosmic shear data from the 208 deg² of the CFHT Legacy Survey. The lines shows various models discussed by Benabed & Bernardeau (40).

2. Fort, B.; Mellier, Y.; 1994 AAR 5, 239.
3. Mellier, Y.; 1999 ARAA 37, 127.
4. Bartelmann, M.; Schneider, P.; 2001 Phys. Rep. 340, 292.
5. Bernardeau, F.; van Waerbeke, L.; Mellier, Y.; 1997 A&A 322, 1.
6. Jain, B.; Seljak, U.; 1997 ApJ 484, 560.
7. van Waerbeke, L.; Bernardeau, F.; Mellier, Y.; 1999 A&A 342, 15.
8. Erben, T.; van Waerbeke, L.; Bertin, E.; Mellier, Y.; Schneider, P.; 2001 A&A 366, 717.
9. van Waerbeke, L.; Mellier, Y.; Erben, T.; et al.; 2000 A&A 358, 30 [vWME+].
10. R. Blandford, A. Saust, T. Brainerd, J. Villumsen; 1991 MNRAS 251, 600
11. Wittman, D.; Tyson, J.A.; Kirkman, D.; Dell'Antonio, I.; Bernstein, G. 2000a Nature 405, 143 [WTK+].
12. Bacon, D.; Réfrégier, A.; Ellis, R.S.; 2000 MNRAS 318, 625 [BRE].
13. Bacon, D.; Réfrégier, A.; Clowe, D.; Ellis, R.S.; 2000 MNRAS 325, 1065 .
14. Kaiser, N.; Wilson, G.; Luppino, G. 2000 preprint, astro-ph/0003338 [KWL].
15. Maoli, R.; van Waerbeke, L.; Mellier, Y.; et al.; 2001 A&A 368, 766 [MvWM+].
16. Rhodes, J.; Réfrégier, A.; Groth, E.J.; 2001 ApJ 536, 79.
17. van Waerbeke, L.; Mellier, Y.; Radovich, M.; et al.; 2001 A&A 374, 757 [vWMR+].
18. Bacon, D., Massey, R., , Réfrégier, A., Ellis, R. 2002. Preprint astro-ph/0203134.
19. Miralda-Escudé, J. 1991 ApJ 380,1
20. Pen, U-L., Van Waerbeke, L., Mellier, Y.; 2002 ApJ 567, 31
21. Kaiser, N. 1992 ApJ 388, 272
22. Kaiser, N. et al., 1994, in Durret et al., *Clusters of Galaxies*, Eds Frontières.
23. Kaiser, N., Squires, G., Broadhurst, T. 1995, ApJ 449, 460.
24. P. Schneider, L. Van Waerbeke, B. Jain, G. Kruse; 1998 ApJ333, 767.

25. A. Réfrégier, J. Rhodes, E. Groth, ApJL, in press, astro-ph/0203131
26. van Waerbeke, L., Mellier, Y, Pelló, R., Pen, U.-L., McCracken, H., Jain, B. 2002, A&A in press. Preprint astro-ph/0 202503
27. Hämerle, H., Miralles, J.-M., Schneider, P., Erben, T., Fosbury, R.A.E.; Freudling, W., Pirzkal, N., Jain, B.; White, S.D.M.; 2002 A&A385 , 743
28. Hoekstra, H., Yee, H., Gladders, M.D. 2001 ApJ 558, L11
29. Hoekstra, H.; Yee, H.; Gladders, M., Barrientos, L., Hall, P., Infante, L. 2002 ApJ 572, 55
30. Pen, U.; van Waerbeke, L.; Mellier, Y.; 2001 ApJ in press astro-ph/0109182.
31. Crittenden, R.G., Natarajan, P.; Pen, U.; Theuns, T. 2001 ApJ 559 , 552.
32. Mackey, J.; White, M.; Kamiionkowski, M.; 2001 preprint, astro-ph/0106364.
33. Hamana, T. et al. 2000. preprint astro-ph/0012200
34. Le Fèvre, O.; Vettolani, P. 2002. SPIE this conference.
35. Schneider, P. 1998 ApJ 498, 43.
36. van Waerbeke, L. 1998 A&A 334, 1.
37. Bernardeau, F., van Waerbeke, L., Mellier, Y. 2002 preprint astro-ph/0201029.
38. Bernardeau, F., Mellier, Y., van Waerbeke, L. 2002 A&A 389, L28.
39. Hoekstra, H., van Waerbeke, L., Gladders, M., Mellier, Y., Yee, H. 2002. Preprint astro-ph/0206103.
40. Benabed, K.; Bernardeau, F.; 2001 preprint, astro-ph/0104371.
41. Miyazaki, S. 2002 in *New Trends in Theoretical and Observational Cosmology*. K. Sato and T. Shiromizu Eds. UAP 2002.
42. Ménard, B., Bartelmann, M. 2002 preprint astro-ph/0203163